Polymer 55 (2014) 505–516

Contents lists available at ScienceDirect

Polymer

journal homepage: www.elsevier.com/locate/polymer

Designing multi-responsive polymers using latent variable methods

Jenny Mayra Guicela Tzoc Torres [b], Emily Nichols [a], John F. MacGregor [a], Todd Hoare [b,*]

[a] ProSensus Inc., 303-1425 Cormorant Road, Ancaster, Ontario L9G 4V5, Canada
[b] Department of Chemical Engineering, McMaster University, 1280 Main Street West, Hamilton, Ontario L8S 4L7, Canada

ARTICLE INFO

Article history:
Received 19 August 2013
Received in revised form
15 December 2013
Accepted 18 December 2013
Available online 27 December 2013

Keywords:
Smart material design
Latent variable models
Polymer optimization

ABSTRACT

The design of stimulus-responsive materials, particularly those intended to respond to more than one stimulus, is an inherently challenging and typically trial-and-error process involving multiple synthesis/characterization iterations in the laboratory. In this work, latent variable models are applied to existing, "failed" polymer formulations and characterizations to facilitate the rational design of materials with specific, targeted properties and to predict responsive polymer properties before synthesizing the materials in the laboratory. The models are capable of simultaneously predicting three targeted polymer properties (cloud point, molecular weight, and % recovery of polymer mass) for poly(*N*-isopropylacrylamide)-based materials that can be reversibly photo-crosslinked. Model inversion and optimization are used to identify new polymer formulations that exhibit significantly improved properties relative to the formulations developed by chemical intuition based on available literature. This model-based design approach moves away from the traditional trial-and-error approach to save time, energy, and resources in the production of novel materials while at the same time generating responsive polymers with improved properties.

1. Introduction

Polymeric materials that exhibit a physical or chemical change in conformation upon the application of a stimulus such as temperature [1–11], light [2,12–20], pH [19,21–23], magnetic field [24,25] or a combination of these [26–33] are referred to as "responsive" or "smart" materials. Smart materials have, in particular, been widely investigated for their potential use as biomaterials [32–37] due to their potential to be triggered within biologically relevant environments. One of the most widely studied responsive materials is poly(*N*-isopropylacrylamide) (poly(NIPAM)), which undergoes a reversible sol-to-gel transition when the surrounding temperature increases above its lower critical solution temperature or "cloud point". The cloud point of a poly(NIPAM) homopolymer is approximately ~32 °C and can be modified higher or lower according to the hydrophilicity or hydrophobicity of any comonomer incorporated in the polymer [34,35]. Comonomers, based on their chemistry, can be included to introduce multiple environmental responses into a single polymer (e.g. pH in addition to temperature) or to introduce reactive residues for subsequent chain functionalization. In this way, both the responses and the functionality of smart materials can be fine-tuned by manipulating the chemistry of the material.

Due to the significant but non-linear impacts of incorporating even very small mole fractions of functional comonomers on both the cloud point and other physicochemical properties of poly(NIPAM)-based polymers, the design of heteropolymers with specific, predictable, and biologically relevant properties is not straightforward. The underlying correlations between the synthesis conditions (e.g. different comonomers, solvents, or chain transfer agents) and the resulting polymer properties have not been widely described, and quantitative predictions have thus far proved elusive. Predictions are particularly challenging given that the synthesis conditions can influence polymer properties in ways that are dependent on each other; for example, a change in solvent will influence both intramolecular interactions between polymer chains and polymer–solvent interactions, resulting in changes in both the phase transition behavior and the molecular weight of the polymer. Additional complexity is introduced in cases where the solvent itself acts as a chain transfer agent. These types of interdependencies are particularly problematic in the design of smart materials for biomedical applications, given the typically narrow range of properties required for materials to be effective.

Our interest lies in the design of dual thermo-responsive and photo-responsive polymers combining the temperature-responsiveness of poly(NIPAM) with the light-responsiveness of cinnamate functional groups. Such materials could quickly gel upon

* Corresponding author. Tel.: +1 905 525 9140x24701.
E-mail address: hoaretr@mcmaster.ca (T. Hoare).

0032-3861/$ – see front matter © 2013 Elsevier Ltd. All rights reserved.
http://dx.doi.org/10.1016/j.polymer.2013.12.041

injection (due to the thermally-driven gelation of the poly(NIPAM)-based copolymers) and then subsequently be covalently crosslinked (or decrosslinked) via light irradiation to dynamically tune gel pore size and stability *in vivo*. Photo-responsive materials have been widely used in medical diagnostics and in ophthalmic therapies, given that light is a safe and easy-to-use external stimuli for physicians [36–38]. Cinnamates are particularly interesting as photo-responsive materials, given that they can form reversible covalent bonds (i.e. crosslinks) upon irradiation with varying wavelengths of ultraviolet light, and can be incorporated into polymers via copolymerization with vinyl cinnamate (VC). Exposing neighboring VCs to wavelengths of ~360 nm causes a *trans–cis* isomerization and [2 + 2] cycloaddition to form a cyclobutane ring (i.e. a cross-link) while exposure to wavelengths of ~250 nm will reverse the chemical crosslinks between VCs [39–43]. However, VC is a highly hydrophobic monomer that significantly reduces the cloud point when incorporated even at small mole fractions in poly(NIPAM)-based polymers. In addition, VC radicals are significantly less reactive than NIPAM; as a result, VC-NIPAM copolymers have significantly lower molecular weights than poly(NIPAM) homopolymers under the same solvent/chain transfer conditions.

For successful implementation of VC-NIPAM copolymers in the targeted biological application, very specific properties are required in the final products. The cloud point must be above room temperature (facilitating easy injection of soluble polymers) but below body temperature to allow the poly(NIPAM) phase transition (and thus thermogelation) to occur *in vivo*. However, the goal of achieving a highly water-soluble polymer conflicts with the hydrophobicity of VC, particularly given that as high a VC fraction as possible is desired to produce a highly photo-responsive material. The number average molecular weight (M_n) is desired to be as high as possible to provide strong and rapid gelation while still being kept below the kidney clearance limit of approximately ~32,000 Da [44] for future excretion of materials *in vivo*. Polymer yields are also desired to be as high as possible, although lower effective polymer yields are often observed when chain transfer agents (used herein to control the molecular weight) are used to prepare polymers.

Given the many variables involved in the polymer synthesis and the conflicting design criteria, trial-and-error experimentation would require numerous costly iterations and would not necessarily result in an optimized or even appropriate formulation. Instead, we seek herein to rationally design polymers by using latent variable models of all previously synthesized polymers related to this work, each of which failed to meet one or more of the stated design criteria. Latent variable models (specifically partial least squares (PLS) models) are an appropriate tool in this case because they seamlessly handle data that is noisy and highly collinear [45], but they are more than a regression tool for less-than-perfect data. Latent variable models provide a framework for extracting insights from whatever historical data is available and building upon it by using designed experiments and optimization in conjunction with the model. For example, latent variable models have been used to reformulate muffin batters [46] and predict properties of polymer blends containing raw materials not previously used in a blend [47,48]. However, the use of latent variable models to improve polymer formulations and reaction conditions for targeted smart materials has not previously been reported.

In this work, a partial least squares (PLS) model is used to represent the previously synthesized polymers. Visualizations of the formulation data and polymer characterizations in this reduced dimensional space (the latent variable space) provide insights into correlations between the variables, the similarities and differences between the synthesized polymers, and the predictive capabilities of the model. Subsequently, the PLS model is inverted to develop iterations of polymerization formulations demonstrated to result in polymers with improved functional properties. The model is updated with new data between iterations, with the second iteration (performed in conjunction with a formal optimization), yielding a polymer that met all of the specified design criteria.

2. Materials and methods

2.1. Materials used

N-isopropylacrylamide (NIPAM) (97.0%, Aldrich Chemicals, Milwaukee, WI, USA) was purified by recrystallization with 60:40 toluene:hexane mixture. Acrylic acid (AA), vinyl cinnamate (VC), thioglycolic acid (TGA), cysteamine hydrochloride (AESH), (all purchased from Sigma–Aldrich, Canada) and dimethyl 2,2′-azobis(2-methylpropionate) (AIBMe) (Wako Chemicals, U.S.A) were used as received. The solvents *N,N*-dimethylformamide (DMF) (99.8%, Caledon Laboratories), tetrahydrofuran (THF) (Fisher Scientific), toluene, hexane, and anhydrous ethanol (EtOH) were all reagent grade (Caledon Laboratories). All water used was of Milli-Q grade.

2.2. Polymer synthesis

Thermo-responsive polymers were prepared by chain transfer free radical polymerization [11,49–52] using the formulations and reaction conditions detailed in Table 1. The term “reactants” refers to all the monomers, chain transfer agents, and initiator used (i.e. all components that may be incorporated into the final polymer).

Briefly, the specified amounts of NIPAM, functional monomer(s) (VC and/or AA), and the desired chain transfer agent (TGA or AESH) were dissolved in the solvent in a round bottom flask equipped with a magnetic stir bar and heated to the given temperature using an oil bath. The flask was covered with aluminum foil to prevent any light exposure to the cinnamate groups during the polymerization. Nitrogen was bubbled through the reaction mixture for 30 min prior to injection of the initiator AIBMe. The polymerization was allowed to proceed according to the times shown in Table 1. For compositions including vinyl cinnamate, unreacted VC and insoluble polymer fractions were isolated by adding the solution dropwise into a beaker (400 mL of H_2O) with a magnetic stir bar and stirring for 48 h; water-soluble polymers remained dissolved while any unreacted hydrophobic VC monomers precipitated and were removed via vacuum filtration. Note that the water insoluble fractions are not relevant to the targeted application (i.e. in the context of the design goals of this paper, the water-insoluble polymer would be considered a “failed” composition); furthermore, accurate cloud point measurements cannot be made on heterogeneous samples. The filtrate was subsequently placed into cellulose dialysis membranes of molecular weight cut off (MWCO) 3,500 Da, dialyzed against fresh water for 8 cycles, lyophilized, and stored. For samples not containing VC, the polymer reaction mixture was rotovapped (to remove excess solvent), added to 200 mL of H_2O, dialyzed against fresh water for 6 cycles using membranes with MWCO values indicated in Table 1 [3,500 Da or 14,000 Da], lyophilized, and stored.

2.3. Polymer composition analysis

Each purified polymer was dissolved at 15 mg/mL in deuterium oxide (D_2O) and evaluated for chemical composition using a Bruker

Table 1
Formulations and properties of the initial 23 polymers (the "historical data").

Formulation number	Chemistry category	X, reactants and reaction conditions												Y, polymer properties		
		NIPAM	AA	VC	AIBMe	TGA	AESH	EtOH	DMF	THF	Reaction temperature	Reaction time	Dialysis membrane MWCO	Cloud point	Avg. No. Mol. Wt., M_n	Recovery
		[g]	[g]	[g]	[g]	[g]	[g]	[mL]	[mL]	[mL]	[°C]	[h]	[Da]	[°C]	[Da]	[%]
1	poly(NIPAM)	10.000	0	0	0.281	0	0.418	0	25.0	0	70	14	14,000	28	11,202	66.30
2	poly(NIPAM)	7.000	0	0	0.100	0	0.200	0	25.0	0	65	17	14,000	28	19,664	54.43
3	poly(NIPAM-AA)	4.999	0.504	0	0.056	0.100	0	25.0	0	0	50	20	14,000		5,248	58.14
4	poly(NIPAM-AA)	4.999	0.504	0	0.056	0.100	0	25.0	0	0	50	20	14,000		4,402	32.70
5	poly(NIPAM-AA)	4.999	0.288	0	0.056	0.100	0	25.0	0	0			14,000	53	2,040	36.88
6	poly(NIPAM-AA)	6.249	0.631	0	0.070	0.125	0	30.0	0	0		20	14,000	61	2,769	55.82
7	poly(NIPAM-AA)	6.249	0.901	0	0.070	0.125	0	30.0	0	0		20	14,000	40	4,269	32.02
8	poly(NIPAM-VC)	3.010	0	0.784	0.046	0	0.045	0	25.0	0	58	12	14,000	23	11,958	16.34
9	poly(NIPAM-VC)	5.002	0	0.610	0.115	0.092	0	0	0	35.0	50	6	14,000	25	4,808	28.34
10	poly(NIPAM-VC)	5.002	0	0.610	0.115	0.092	0	0	35.0	0	50	6	3,500	23	6,894	18.89
11	poly(NIPAM-VC)	5.002	0	0.610	0.115	0.092	0	35.0	0	0	50	6	3,500	27	2,189	9.98
12	poly(NIPAM-VC)	5.092	0	0.871	0.069	0	0.045	35.0	0	0	50	24	14,000	23	4,016	1.84
13	poly(NIPAM-VC)	5.205	0	1.394	0.035	0	0.023	40.0	0	0	50	24	14,000	18	9,776	3.79
14	poly(NIPAM-VC-AA)	3.746	0.541	1.307	0.046	0.074	0	20.0	0	0	55		3,500	38	1,438	4.47
15	poly(NIPAM-VC-AA)	3.746	0.541	1.307	0.046	0.074	0	0	0	20.0	50	6	3,500	38	1,542	1.61
16	poly(NIPAM-VC-AA)	3.746	0.541	1.307	0.046	0.074	0	0	20.0	0	50	6	3,500		1,609	4.47
17	poly(NIPAM-VC-AA)	3.746	0.541	1.307	0.046	0.074	0	7.5	0	7.5	50	6	3,500		1,517	1.07
18	poly(NIPAM-VC-AA)	3.746	0.541	1.307	0.046	0.074	0	7.5	7.5	0	50	6	3,500		1,483	3.22
19	poly(NIPAM-VC-AA)	3.746	0.541	1.307	0.046	0.074	0	0	7.5	7.5	50	6	3,500	29	1,470	2.15
20	poly(NIPAM-VC-AA)	3.746	0.541	1.307	0.046	0	0.074	0	15.0	0	60	12	3,500	37	2,225	2.86
21	poly(NIPAM-VC-AA)	5.680	0.363	1.315	0.046	0.014	0	40.0	0	0	50	24	14,000	43	2,173	1.50
22	poly(NIPAM-VC-AA)	5.703	0.454	1.098	0.046	0	0.034	40.0	0	0	50	24	14,000	36	2,937	0.69
23	poly(NIPAM-VC-AA)	5.726	0.307	1.062	0.023	0	0.045	40.0	0	0	50	24	14,000		3,582	0.11

200 MHz nuclear magnetic resonance spectrometer operating at room temperature. The molar quantities of each monomer incorporated into the polymer were subsequently calculated by integrating the characteristic peak areas related to the protons from each monomer.

2.4. Cloud point measurements

The cloud point temperature was determined spectrophotometrically by measuring the % transmittance of light at $\lambda = 500$ nm while increasing the temperature of the polymer solutions. Each polymer was dissolved in 10 mM PBS at a concentration of 10 %w/v. All solutions were placed in polystyrene cuvettes and agitated for 20 s using a vortex operating at 2500 rpm before each measurement. The sample cells were subjected to heating from 10 °C to 65 °C, with 3 °C increments and 5-min equilibration times between measurements. The cloud point reported is the midpoint value (inflection point) of the phase transition between the pre- and post-plateau regions of transmittance–temperature curve.

2.5. Number average molecular weight measurements

Polymer molecular weight (M_n) was measured using gel permeation chromatography (GPC, Waters) incorporating a Waters 2414 refractive index detector and a Waters 717 Plus autosampler. Polymers were dissolved at 7 mg/mL in THF, filtered, and then loaded on a Styragel Column, HR2 (5 μm, 7.8 mm × 300 mm) run at a flow rate of 1.0 mL/min THF at 35 °C. Values of M_n reported for each sample were calculated based both on narrow polydispersity polystyrene standards (Waters) and broader polydispersity poly(-NIPAM) standards (PolymerSource and Sigma–Aldrich) with M_n ranging from ~2,000 Da to 125,000 Da. The poly(NIPAM) samples were chosen to calibrate the experimental polymer molecular weights given the chemical similarity of these standards to the polymers being analyzed.

2.6. Recovery measurements

The recovered mass of each polymer was measured gravimetrically by weighing the lyophilized product recovered. Polymer recoveries are expressed as a wt% relative to the sum of the monomer masses in that formulation.

2.7. Statistical analysis methods

The latent variable modeling was performed using ProSensus MultiVariate (ProMV) version 12.08 (ProSensus Inc.). Matlab version 2011b (The Mathworks Inc.) was used to run ProSensus' optimization algorithm for model-based formula development in Iteration 2.

3. Results & discussion

3.1. Design and analysis of initial 23 formulations

The initial 23 polymer formulations were designed based on a literature survey of phase transition temperatures of functionalized poly(NIPAM) polymers [11,49–52]. Each polymer falls into one of the following general categories: (1) homopolymer poly(*N*-isopropylacrylamide) (poly(NIPAM)), for reference, (2) acrylic acid-NIPAM copolymers (poly(NIPAM-AA)), requiring subsequent grafting reactions to attach pendant cinnamate groups, (3) vinyl cinnamate-NIPAM copolymers (poly(NIPAM-VC)), or (4) acrylic acid-co-vinyl cinnamate-co-NIPAM terpolymers (poly(NIPAM-VC-AA)).

In each polymer, NIPAM was the majority monomer in order to target a cloud point between room temperature (~25 °C) and body temperature (~37 °C), and to maintain thermo-crosslinking capability. The fractions of AA (to increase polymer solubility in PBS buffer) and/or VC (to incorporate the light-sensitive cinnamate residues) were varied together with the solvent type (EtOH, DMF, or THF) and chain transfer agent (AESH: amine-terminated or TGA: carboxylic acid-terminated) to attempt to synthesize polymers with the targeted properties. Fig. 1 shows the general free radical polymerization reaction of a typical poly(NIPAM-VC-AA) polymer.

The chemical composition of the polymers was assessed by nuclear magnetic resonance spectroscopy. The theoretical and measured monomer mole fractions in the different polymers produced are shown in Table 2.

Note that acrylic acid is incorporated quantitatively into copolymers with NIPAM while vinyl cinnamate incorporations lie well below the amount of monomer added to the reaction vessel. This is expected because of the significantly slower reactivity of VC relative to AA and NIPAM and presents another challenge in the design of polymers with desired target properties. However, in general, the more of any monomer is added to the reaction mixture, the more of that monomer is incorporated into the resulting polymer, indicating a correlation between the polymer formulation and composition.

The measured target properties (cloud point, molecular weight, and recovery) for the initial 23 formulations are shown in Fig. 2. Several of the polymers containing VC (the photo-responsive group) have cloud points in or near the desired temperature range, but they also exhibit very low polymer recoveries and generally very low M_n values relative to the target properties.

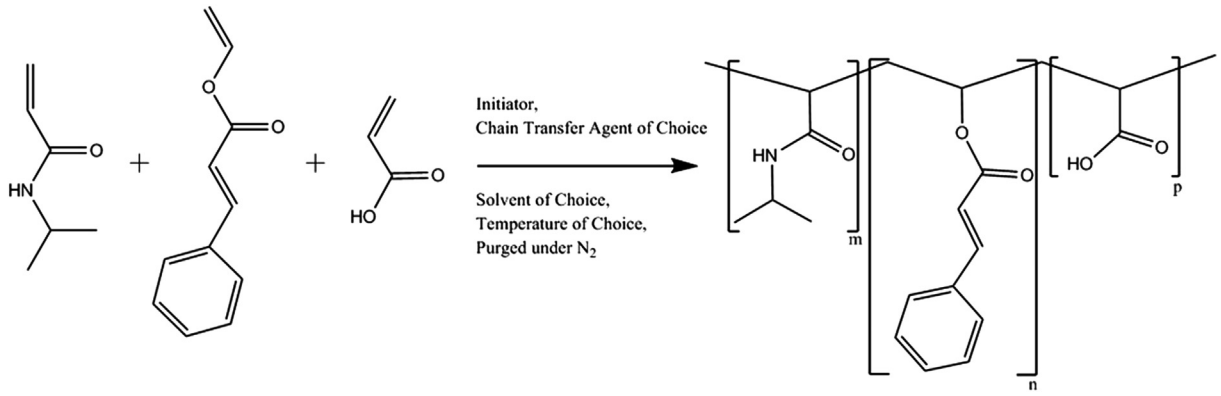

Fig. 1. Schematic representation of the polymerization reaction to obtain poly(NIPAM-VC-AA).

Table 2
Theoretical and measured mole fractions of monomers in polymers produced (mole fractions calculated on a monomer-only basis).

Formulation number	Chemistry category	NIPAM incorporated [mol NIPAM/sum monomers]%		AA incorporated [mol AA/sum monomers]%		VC incorporated [mol VC/sum monomers]%	
		Theoretical	Measured	Theoretical	Measured	Theoretical	Measured
5	poly(NIPAM-AA)	91.7	92.1	8.3	7.9	0	0
7	poly(NIPAM-AA)	81.5	82.6	18.5	17.4	0	0
8	poly(NIPAM-VC)	85.5	97.0	0	0	14.5	3.0
9	poly(NIPAM-VC)	92.7	96.8	0	0	7.3	3.2
16	poly(NIPAM-VC-AA)	68.8	90.0	15.6	6.2	15.6	3.8
19	poly(NIPAM-VC-AA)	68.8	83.4	15.6	13.2	15.6	3.4

Therefore, none of the initial 23 formulations were deemed successful according to the design criteria. Such challenges are common in the design of smart copolymers since both hydrophilic and hydrophobic comonomers strongly affect the product solubility, phase transition, chain length, and amount of material recovered. Note that the poly(NIPAM)-only samples exhibited all of the target properties but without the required functionality of the light-responsive functional groups introduced by vinyl cinnamate, as anticipated.

3.2. Organizing the data for multivariate analysis

To subject the data collected via this initial trial-and-error strategy to multivariate statistical analysis, data for the initial 23 polymers (hereafter referred to as the "historical data") was organized into a concise tabular format. This database-style format is the foundation for extracting knowledge from all past development data using latent variable methods. For formulation variables, zeros were filled in wherever an ingredient was not used. Missing values were left as empty cells because latent variable methods inherently handle missing data [45] (observations with missing values need not be excluded). The model's utility and interpretability are affected by the choice of units used to express the variables. Each monomer, initiator, and chain transfer amount is expressed as a mole percentage of the total moles of reactants used in the polymerization. The solvent volumes used were divided by the total number of moles of reactants used to represent both the total amount of solvent used as well as the concentration of reagents in each polymerization recipe. The term "reactants" refers to all the monomers, chain transfer agents, and initiator used (i.e. all components that may be incorporated into the final polymer). It is important to note that the input variables are not independent. For example, the mole fractions of all monomers must sum to one, and the chosen solvent's boiling point imposes a limitation on reaction temperature. Latent variable methods can handle these correlations because the data is being projected into a lower dimensional, orthogonal space before it is used for calculating predictions.

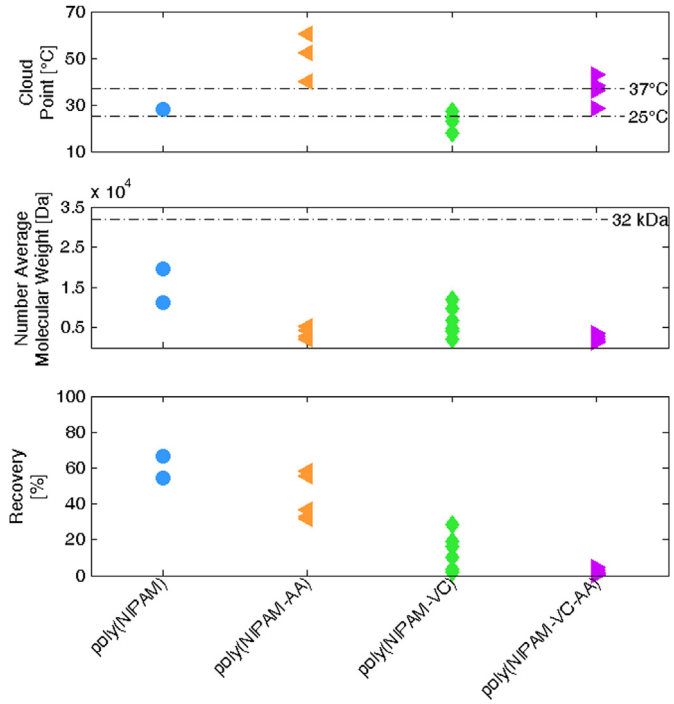

Fig. 2. Polymer properties of the initial 23 formulations.

3.3. Model 1: PLS model of historical data

A PLS model was built using the historical data in order to explore correlations among the variables and assess the predictability of the polymer properties. The model contains five latent variables, with an overall R^2Y value of 0.825 and an overall Q^2Y value of 0.675, as shown in Fig. 3(a). R^2Y has the same meaning here as R^2 in ordinary least squares regression; it is a measure of how well the model fits the Y-data (cloud point, number average molecular weight, and recovery). PLS also models the X-space and therefore R^2X can also be calculated; a high R^2X is desired when the model will be inverted to estimate the X variables required to achieve a set of Y properties. Q^2Y is a measure of the model's predictive capability, calculated using cross-validation. R^2 and Q^2 can also be calculated individually for each Y-variable as shown in Fig. 3(b).

Practically speaking, these R^2 and Q^2 values demonstrate that the majority of the information in the historical data (12 dimensions in X, 3 dimensions in Y) can be summarized in a 5-dimensional latent variable space, or model space, which is much easier to interpret. In a PLS model, the first latent variable is the direction of greatest covariance between X and Y, and each successive model dimension explains less covariance. Here, while the third dimension is statistically significant by cross validation, it captures much less information than the first two dimensions (see Fig. 3). Therefore, a loading bi-plot of just the first two model dimensions, shown in Fig. 4, captures the most important relationships between the variables and observations.

PLS loading bi-plots show the relationships among and between observations and variables. Observations cluster together because of their similarities, in this case their chemistry type. Because mean-centering is a standard pre-processing step for PLS, the origin represents the average observation in the model. The locations of the variables relative to the observations indicate why the observations fall where they do. For example, Fig. 4 reinforces that polymers containing VC (green and magenta symbols (in web version), located closest to VC) had the lowest recoveries (i.e. they are the observations located furthest from recovery).

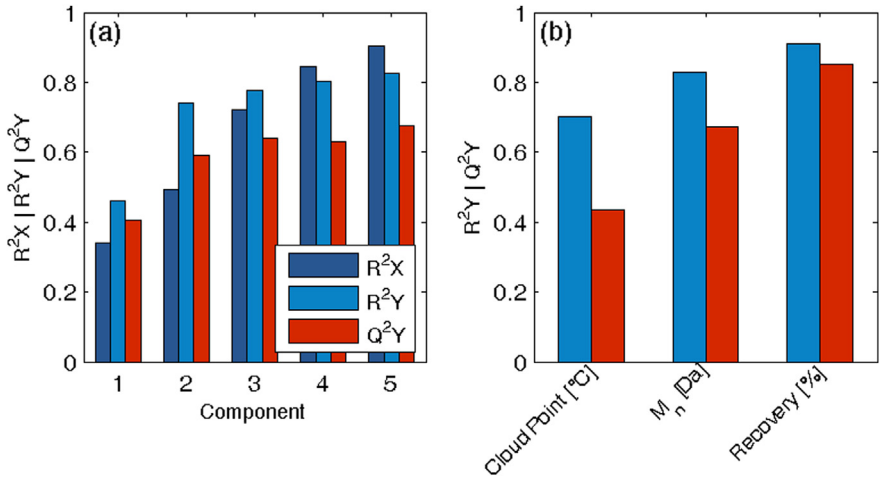

Fig. 3. (a) Cumulative R^2X, R^2Y, and Q^2Y for the PLS model of the historical data; (b) R^2Y and Q^2Y for each of the target properties (*Y*-variables based on the three latent variable Model 1).

Loading bi-plots also indicate relationships among variables. Variables that sit close together in the latent variable space are positively correlated, while variables located opposite each other are negatively correlated. For example, by comparing the positions of each of the solvents relative to M_n, it is evident that reactions completed in DMF rather than EtOH or THF resulted in polymers with higher M_n and higher recovery. AESH is located near M_n, whereas TGA is located diagonally across the origin; as such, if the goal is to increase molecular weight while still using a chain transfer agent, AESH should be used preferentially. Note that no polymers prepared in the absence of chain transfer agents are included in the historical data, resulting in the least efficient chain transfer agent (AESH) being associated with high molecular weights as opposed to both chain transfer agents being negatively correlated with molecular weight. TGA is located near cloud point while AESH is located in the opposite quadrant of the plot, which means that the use of TGA rather than AESH as the chain transfer agent tends to produce polymers with a higher cloud point. Since both chain transfer agents are hydrophilic in nature, this observation is likely attributed to the reduced chain length of TGA-mediated polymers (associated with a less cooperative phase transition which would require a higher temperature to complete [53]) rather than a hydrophobicity effect.

Of note, recovery and M_n are positively correlated in the first latent variable but negatively correlated in the second latent variable, an apparently contradictory result. Since the first latent variable in a PLS model is the direction of greatest covariance, the positive correlation can be thought of as a macro trend while the negative correlation is associated with a more subtle effect. Fig. 5 shows that a negative correlation is observed between recovery and molecular weight within each polymer group (likely due to the effect of molecular weight on polymer solubility) but an overall positive correlation is observed when all chemistries are plotted together. Since VC is negatively correlated with both molecular weight and recovery, it is likely the influence of VC on both limiting chain length (due to its slower polymerization kinetics) and reducing the recovery (by increasing the hydrophobicity of the chain and thus promoting precipitation) that results in the overall

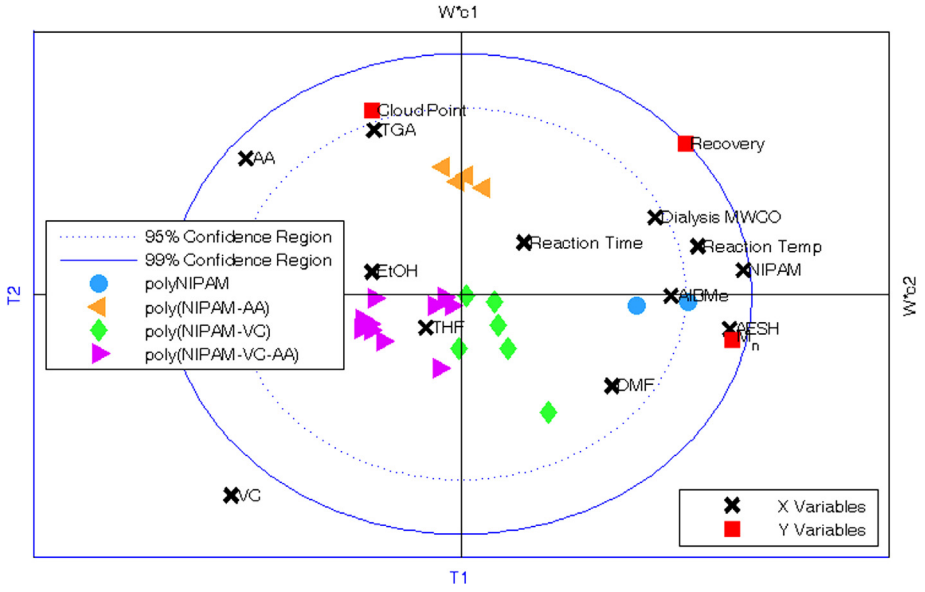

Fig. 4. Loading bi-plot for PLS of historical data.

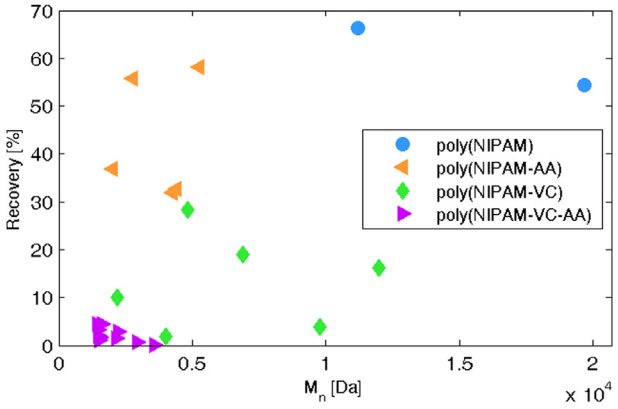

Fig. 5. Recovery versus M_n for the initial 23 formulations.

positive correlation observed between recovery and M_n. These examples illustrate the power of latent variable methods for analyzing systems with many competing effects on the material properties of a specific polymer system.

3.4. Model inversion

PLS approaches provide a model for both the *X*-space and the *Y*-space; therefore, it is possible to invert the PLS model and predict the values of the *X*-variables needed to produce a material with some desired characteristics *Y*. The Model Explorer tool in the ProMV software used to perform this analysis allows the user to "drag" a new observation around the latent variable space and view the corresponding values of the *X* and *Y*-variables. This is an unconstrained model inversion, and the user can take the resulting *X*-variable values and adjust them slightly to meet any required constraints. In this case, for example, the mole fractions of the reactants must be adjusted to sum to one, and any negative values must be assigned to zero.

Four new polymers were synthesized and characterized based on formulations identified by the inversion of Model 1. Table 3 shows the formulations and properties of the four new polymers synthesized.

The theoretical and measured monomer mole fractions in the different polymers produced are shown in Table 4. Analogously to the historical polymers, AA incorporates better than the VC; however, the % VC incorporation with respect to the amount of VC charged is higher in these iteration polymers.

Fig. 6(a), (b) and (c) compares the model-predicted and actual values of cloud point, M_n, and recovery respectively for both the historical data (the "training" data set for this model) and the four new polymers ("Iteration 1"). Fig. 6(d) shows the squared prediction error (SPE-X) for the same data points. Three of four Iteration 1 formulas have SPE-X values that are below the 99% confidence level for the model; this means that the relationships that were present between the *X*-variables in the historical data have been maintained to a degree that is acceptable for predicting the polymer properties.

Fig. 6 suggests that Model 1 can effectively predict the desired polymer properties for three of four of the new (Iteration 1) formulations within the SPE-X confidence limits. In particular, the root mean-squared error of prediction for the Iteration 1 formulations is 3 °C for cloud point and 23 wt% for recovery. The goodness of fit observed for cloud point is particularly noteworthy since the thermal phase transition can occur over both narrow and broad temperature ranges depending on the mix of comonomers used. The model's prediction of M_n is less accurate,

Table 3
Iteration 1 formulations developed by unconstrained model inversion and manual adjustments.

Formulation number	Chemistry category	*X*, reactants and reaction conditions												*Y*, polymer properties		
		NIPAM	AA	VC	AIBMe	TGA	AESH	EtOH	DMF	THF	Reaction temperature	Reaction time	Dialysis membrane MWCO	Cloud point	Avg.No.Mol. Wt., M_n	Recovery
		[g]	[g]	[g]	[g]	[g]	[g]	[mL]	[mL]	[mL]	[°C]	[h]	[Da]	[°C]	[Da]	[%]
24	poly(NIPAM-VC-AA)	6.000	0.353	0.706	0.028	0	0.014	56.3	0	0	50	15	3,500	30	4,117	0.14
25	poly(NIPAM)	2.000	0	0	0.015	0	0.005	0	56.3	0	65	15	14,000	28	19,522	80.00
26	poly(NIPAM-VC-AA)	6.500	1.200	1.178	0.044	0	0.018	0	49.3	0	65	16	3,500	45	1,773	2.25
27	poly(NIPAM-VC)	6.000	0	0.961	0.014	0	0.033	0	0	59.5	50	15	14,000	22	19,775	2.11

Table 4
Theoretical and measured mole fractions of monomers in Iteration 1 polymers produced (mole fractions calculated on a monomer-only basis).

Formulation number	Chemistry category	NIPAM incorporated [mol NIPAM/sum monomers]%		AA incorporated [mol AA/sum monomers]%		VC incorporated [mol VC/sum monomers]%	
		Theoretical	Measured	Theoretical	Measured	Theoretical	Measured
24	poly(NIPAM-VC-AA)	85.6	NA[a]	7.9	NA[a]	6.5	NA[a]
25	poly(NIPAM)	100.0	100.0	0	0	0	0
26	poly(NIPAM-VC-AA)	71.0	70.7	20.6	24.9	8.4	4.4
27	poly(NIPAM-VC)	90.6	95.4	0	0	9.4	4.6

[a] Note: Formulation 24 did not allow for sufficient material recovery to perform the NMR measurements.

meaning that M_n is not a linear function of the process variables. This is physically consistent with the multiple factors that may contribute to M_n values (e.g. chain transfer to chain transfer agent, chain transfer to solvent, differing copolymerization ratios among the comonomers, and different affinities for termination by combination versus disproportionation in different solvents or for different monomer combinations). However, while accurate quantitative predictions were not achieved in Iteration 1, the two Iteration 1 materials predicted by the model to have a higher M_n did exhibit significantly higher M_n values experimentally, a positive outcome given that achieving a higher M_n for VC-containing copolymers was a key objective in the design of improved copolymers. Thus, while the observed versus predicted fit for molecular weight is imperfect, the latent variable approach can still be effectively used to identify formulations with improved properties.

3.5. Model 2: PLS model updated after Iteration 1

To improve the model (particularly the predictions of M_n), data from Iteration 1 was appended to the historical data, and an updated model was constructed. Therefore, the "training" data for Model 2 includes both the historical data and the data from Iteration 1.

The updated model had an overall R^2Y 0.812 and overall Q^2Y 0.660 and could simultaneously predict each of the three target properties with high individual R^2 and Q^2 values, as shown in Fig. 7. This improvement in predictability (particularly of cloud point and M_n) was achieved since the Iteration 1 formulations resulted in polymers with significantly higher molecular weight than the historical data and thus significantly expanded the range and "knowledge" of the model in terms of what factors influence molecular weight.

Analysis of the model coefficients (Fig. 8) indicates the size and direction of each *X*-variable's influence on each *Y*-variable. The model results correspond well with the physical realities of the copolymerizations performed. For example, cloud point is positively correlated primarily with AA (increased chain hydrophilicity), and TGA (decreased chain length) but negatively correlated with VC (increased chain hydrophobicity). M_n is positively correlated with NIPAM (higher propagation rate than AA or VC) and MWCO of the membrane used to purify the product (larger MWCO leads to the removal of more smaller chains and retains only the largest chains). M_n is negatively correlated with AIBMe (increased number of chains

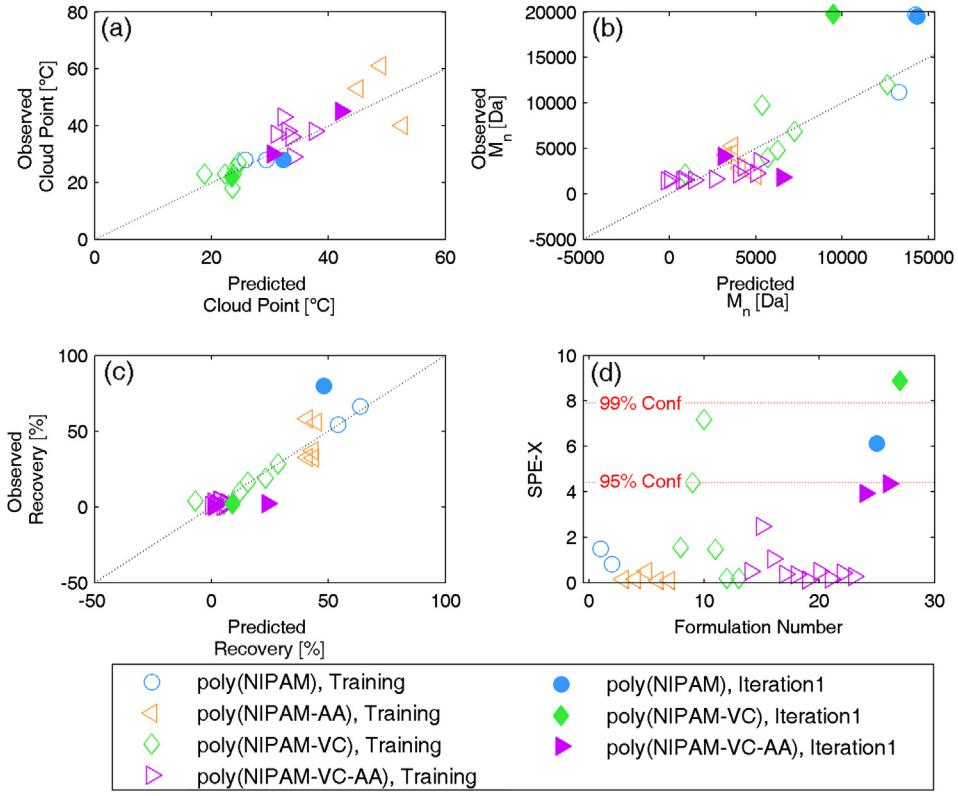

Fig. 6. Observed versus predicted values for (a) cloud point, (b) M_n, and (c) recovery for the historical observations (unfilled points) and Iteration 1 (filled points). (d) SPE-X values for the same observations.

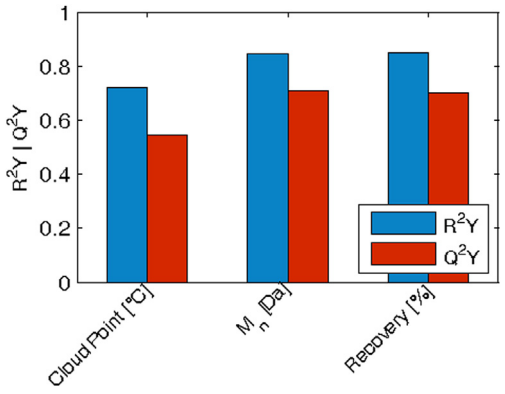

Fig. 7. R^2Y and Q^2Y for model 2.

initiated), AA (lower propagation rate than NIPAM [53]), and the use of ethanol (potential chain transfer to solvent). Recovery is most negatively correlated with VC (reduced polymer solubility) while being positively correlated with the use of TGA.

3.6. Optimization in the latent variable space

To develop formulations that would better satisfy the design criteria, inversion of Model 2 was pursued using formal constrained optimization methods. The chemistry of poly(NIPAM-VC-AA) was targeted for optimization since it is the most desirable from a design standpoint; that is, it does not require subsequent grafting reactions to attach light-sensitive cinnamate groups. The objective function of the optimization targeted cloud points between 30 °C and 37 °C while maximizing M_n and recovery. The objective function also contained penalty terms for SPE-X and Hotelling's T^2; these ensured that the new formulations stayed within the subspace of the latent variable model, essentially preventing excessive extrapolation. Constraints were used to enforce feasible values of all reactants and conditions (including all the reagent mole fractions adding to one) and a minimum proportion of VC to ensure sufficient light-responsive crosslinking functionality. The new formulation 28 (Iteration 2) recipe and properties are shown in Table 5.

The theoretical and measured monomer mole fractions in the polymer are shown in Table 6. The optimized formulation 28 has a significantly higher amount of VC incorporated into the polymer compared to the historical polymers. Molar amounts of each monomer are higher and closer to their theoretical values of incorporation, not readily achieved in the past formulations.

Fig. 9 shows the squared prediction error (SPE-X) for both the training data for Model 2 and the Iteration 2 formulation (formulation 28) identified via the optimization process. While the SPE-X values for Model 2's training data are within the 99% confidence limit, the new formulation developed by constrained optimization has a significantly higher value. This means that the optimized formulation is significantly different from any previous formulations in terms of correlation structure among *X*-variables. On this basis, the model-predicted properties of this formulation may be inaccurate in terms of absolute values. However, the model provides a basis for moving the desired properties of the polymers in the right direction, i.e. towards desirable combinations of targeted properties.

The score plot in Fig. 10 shows the position of all the polymers synthesized (including the optimized formulation 28 resulting from Iteration 2, the filled triangle). Note that formulations within each chemistry category in the training data are clustered in the latent variable space; as such, continued trial-and-error experimentation would likely only explore formulations within or near

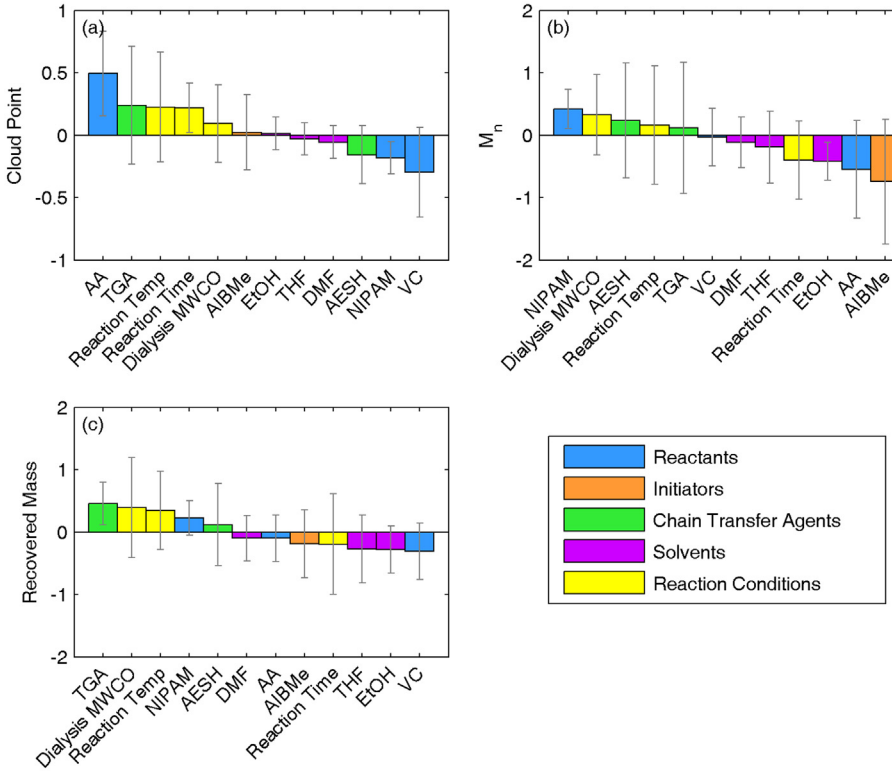

Fig. 8. Coefficient plots for Model 2, showing the influence (scaled magnitude and direction) of each *X*-variable on each *Y*-variable: (a) cloud point; (b) M_n; (c) recovery. These coefficients apply to mean-centered and scaled data, i.e. the effects shown are relative to the average observation in the model.

Table 5
Iteration 2 formulation developed using constrained model inversion of Model 2.

Formulation number	Chemistry category	*X*, reactants and reaction conditions												*Y*, polymer properties		
		NIPAM	AA	VC	AIBMe	TGA	AESH	EtOH	DMF	THF	Reaction temperature	Reaction time	Dialysis membrane MWCO	Cloud point	Avg.No.Mol. Wt., M_n	Recovery
		[g]	[g]	[g]	[g]	[g]	[g]	[mL]	[mL]	[mL]	[°C]	[h]	[Da]	[°C]	[Da]	[%]
28	poly(NIPAM-VC-AA)	7.052	0.388	1.072	0.167	0	0.382	0	75.1	0	70	30	14,000	36	2,982	18.6

Table 6
Theoretical and measured mole fractions of monomers in optimized Iteration 2 polymer produced (mole fractions calculated on a monomer-only basis).

Formulation number	Chemistry category	NIPAM incorporated [mol NIPAM/sum monomers]%		AA incorporated [mol AA/sum monomers]%		VC incorporated [mol VC/sum monomers]%	
		Theoretical	Measured	Theoretical	Measured	Theoretical	Measured
28	poly(NIPAM-VC-AA)	84.4	80.2	7.3	8.9	8.3	10.9

these clusters, most likely leading to continued generation of poor-to-average target properties. In contrast, the optimized formulation lies far from its parent chemistry cluster. Without the use of the model, it is unlikely that it would be identified as candidate formulation. Of note, the optimized formulation 28 lies close to the NIPAM-only homopolymers in Fig. 10, consistent with the successful incorporation of a large fraction of VC comonomer without significantly changing the phase transition behavior of the polymer.

The successful optimized poly(NIPAM-VC-AA) (formulation 28) exhibited a cloud point in the desired range (36 °C), together with an acceptable value of M_n (nearly 3,000 Da) and significantly higher mass recovery than had been achieved with other formulations in the same chemistry family (~1.6 g or 19 wt%). Among the twelve previous formulations of poly(NIPAM-VC-AA), only four exhibited a cloud point in the desired range (listed in Table 7); however, each failed to achieve one or more of the other required properties. For example, formulation 24 had the highest molecular weight within the polymer family but exhibited a very poor recovery, while formulations 19 and 20 had slightly better product recovery but lower than desired molecular weights. Formulation 28 exhibited almost a 10-fold improvement in recovery over formulation 20 and an increased M_n that would make this polymer relevant for the desired application.

3.7. Model 3: final model update

An updated model (Model 3) was constructed that contained all of the data from Tables 1, 3, 5, and the additional formulations in Table S1 of the Supplementary data (i.e. Historical Data, Iteration 1, Iteration 2, and four other polymers). Plots for this model are provided in the Supplementary data, Figure S1 and Figure S2. Based on the larger sample space, Model 3 exhibits a broader understanding of the effects of reactant concentrations and reaction conditions on polymer properties than Model 2, given the additional sample space studied with the additional formulations included. Model 3 suggests that polymerization formulations that use less chain transfer agent and VC, more NIPAM, DMF as the reaction solvent, and larger dialysis MWCO lead to polymers with longer chains. High reaction temperatures and high amounts of NIPAM lead to higher product recovery while high amounts of VC or EtOH usage lead to less polymer recovered. Higher amounts of AA or TGA, longer reaction times, and increased temperature help increase cloud point while higher amounts of NIPAM and VC and the use of DMF or THF decrease cloud point. Many of these relationships are easily explained, or even obvious, based on knowledge of the chemicals involved. However, the latent variable approach quantifies the effect of each reactant and reaction condition on each of the polymer properties, easily handles the inherent correlations, and provides a formal framework for optimizing the desired characteristics. This technique can dramatically reduce the number of trials required to reach a successful formulation, particularly in scenarios with competing design criteria. It should be noted that significantly fewer than 23 initial

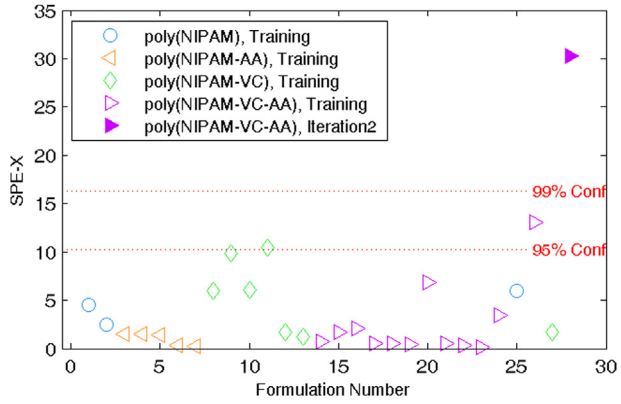

Fig. 9. SPE-X for Model 2 training data (unfilled points) and the optimized ("Iteration 2") formulation (filled point).

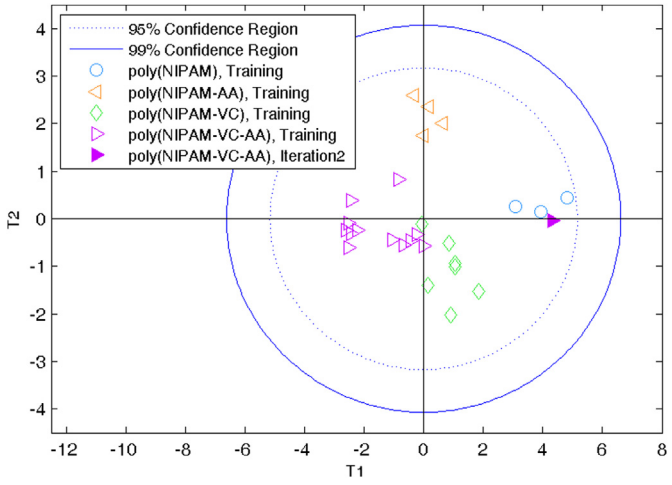

Fig. 10. Score plot showing Model 2 training data (unfilled points) and the optimized ("Iteration 2") formulation (filled point).

Table 7
Comparison of best poly(NIPAM-VC-AA) formulations.

Formulation number	Data set	Cloud point [°C]	M_n [Da]	Recovered mass [g]
19	Historical Data	29	1,470	0.12
20	Historical Data	37	2,225	0.16
22	Historical Data	36	2,937	0.05
24	Iteration 1	30	4,117	0.01
28	Iteration 2	36	2,982	1.58

polymerizations need to be done to achieve similar results using this model-driven approach; the 23 initial recipes were synthesized before the idea to use latent variable methods was related to this work. In this case, while 23 polymers prepared using the trial-and-error approach did not successfully meet all of the design criteria, a polymer with the target properties was achieved after only five model-driven samples were prepared.

4. Conclusions

Designing responsive materials can be challenging due to the conflicting and interacting influences of different input variables on the material properties. Applying latent variable methods to polymerization reaction data is a rational approach to designing novel responsive materials, and is far superior to the inefficient trial-and-error approach typically used for novel material development. All past polymer data was useful in building PLS models, including data from "failed" polymers that exhibited poor properties outside of the target range for a specific application. Even challenging non-linear relationships among variables, datasets with missing data, and highly correlated data can be modeled effectively using latent variable methods. Specifically, a polymer with a cloud point of ~36 °C with M_n ~3,000 Da and recovery 10-fold higher than the next best polymerization recipe of a similar chemistry was designed through numerical optimization of the latent variable model. This new polymer exhibited a superior suite of properties not easily or quickly achievable through multiple trial-and-error iterations. The same approach could be used for the design of other smart polymers with application-specific target properties.

Acknowledgments

The 20/20 NSERC Ophthalmic Materials Network and the NSERC ENGAGE grant (with ProSensus Inc.) are acknowledged for financial support. ProSensus Inc. is thanked for both technical help and generous permission to use ProMV software. Nick Burke is acknowledged for his assistance with GPC analysis, Janine Ho is acknowledged for performing preliminary cloud point trials, and Sahar Mokhtari is acknowledged for her assistance with NMR.

Appendix A. Supplementary data

Supplementary data related to this article can be found online at http://dx.doi.org/10.1016/j.polymer.2013.12.041.

References

[1] Heskins M, Guillet JE. Solution properties of poly(N-isopropylacrylamide). J Macromol Sci Part A Chem 1968;2:1441–55.
[2] Budhlall BM, Marquez M, Velev OD. Microwave, photo- and thermally responsive PNIPAm–gold nanoparticle microgels. Langmuir 2008;24:11959–66.
[3] Hoare T, Pelton R. Highly pH and temperature responsive microgels functionalized with vinylacetic acid. Macromolecules 2004;37:2544–50.
[4] Garcia A, Marquez M, Cai T, Rosario R, Hu Z, Gust D, et al. Photo-, thermally, and pH-responsive microgels. Langmuir 2007;23:224–9.
[5] Radhakumary C, Antonty M, Sreenivasan K. Drug loaded thermoresponsive and cytocompatible chitosan based hydrogel as a potential wound dressing. Carbohydr Polym 2011;83:705–13.
[6] Mallikarjuna N, Rao KMS, Prasad CV, Rao KC, Rao KSVK, Subha MCS. Synthesis, characterization and use of poly(N-isopropylacrylamide-co-N-vinylcaprolactam) crosslinked thermoresponsive microspheres for control release of ciproflaxin hydrochloride drug. J Appl Pharm Sci 2011;01:171–7.
[7] Nolan CM, Serpe MJ, Lyon LA. Thermally modulated insulin release from microgel thin films. Biomacromolecules 2004;5:1940–6.
[8] Hoare T, Pelton R. Calorimetric analysis of thermal phase transitions in functionalized microgels. J Phys Chem B 2007;111:1334–42.
[9] Hoare T, Sivakumaran D, Stefanescu CF, Lawlor MW, Kohane DS. Nanogel scavengers for drugs: local anesthetic uptake by thermoresponsive nanogels. Acta Biomaterialia 2012;8:1450–8.
[10] Tan BH, Pelton RH, Tam KC. Microstructure and rheological properties of thermo-responsive poly (N-isopropylacrylamide) microgels. Polymer 2010;51:3238–43.
[11] Ha DI, Lee SB, Chong MS, Lee YM, Kim SY, Park YH. Preparation of thermo-responsive and injectable hydrogels based on hyaluronic acid and poly(N-isopropylacrylamide) and their drug release behaviors. Macromol Res 2006;14:87–93.
[12] He J, Zhao Y. Light-responsive polymer micelles, nano- and microgels based on the reversible photodimerization of coumarin. Dyes Pigments 2011;89:278–83.
[13] Peng K, Tomatsu I, Kros A. Light controlled protein release from a supramolecular hydrogel. Chem Commun 2010;46:4094–6.
[14] Trenor SR, Shultz AR, Love BJ, Long TE. Coumarins in polymers: from light harvesting to photo-cross-linkable tissue scaffolds. Chem Rev 2004;104:3059–77.
[15] Jiang HY, Kelch S, Lendlein A. Polymers move in response to light. Adv Mater 2006;18:1471–5.
[16] Katz JS, Burdick JA. Light-responsive biomaterials: development and applications. Macromol Biosci 2010;10:339–48.
[17] Zhang H-J, Xin Y, Yan Q, Zhou L-I, Peng L, Yuan J-Y. Facile and efficient fabrication of photoresponsive microgels via thiol–Michael addition. Macromol Rapid Commun 2012;33:1952–7.
[18] Tomatsu I, Peng K, Kros A. Photoresponsive hydrogels for biomedical applications. Adv Drug Deliv Rev 2011;63:1257–66.
[19] Andreopoulos FM, Persaud I. Delivery of basic fibroblast growth factor (bFGF) from photoresponsive hydrogel scaffolds. Biomaterials 2006;27:2468–76.
[20] Wells LA, Brook MA, Sheardown H. Generic, anthracene-based hydrogel crosslinkers for photo-controllable drug delivery. Macromol Biosci 2011;11:988–98.
[21] Schmaljohann D. Thermo- and pH-responsive polymers in drug delivery. Adv Drug Deliv Rev 2006;58:1655–70.
[22] Zhao C, Gao X, He P, Xiao C, Zhuang X, Chen X. Facile synthesis of thermo- and pH-responsive biodegradable microgels. Colloid Polym Sci 2011;289:447–51.
[23] Hoare T, Pelton R. Titrametric characterization of pH-induced phase transitions in functionalized microgels. Langmuir 2006;22:7342–50.
[24] Hoare T, Timko BP, Santamaria J, Goya GF, Irusta S, Lau S, et al. Magnetically triggered nanocomposite membranes: a versatile platform for triggered drug release. Nano Lett 2011;11:1395–400.
[25] Hoare T, Santamaria J, Goya GF, Irusta S, Lin D, Lau S, et al. A magnetically triggered composite membrane for on-demand drug delivery. Nano Lett 2009;9:3651–7.
[26] Zha L, Banik B, Alexis F. Stimulus responsive nanogels for drug delivery. Soft Matter 2011;7:5908–16.
[27] Liu F, Urban MW. Recent advances and challenges in designing stimuli-responsive polymers. Progr Polym Sci 2010;35:3–23.
[28] YongYong L, HaiQing D, Kang W, DongLu S, XianZheng Z, RenXi Z. Stimulus-responsive polymeric nanoparticles for biomedical applications. Sci China Chem 2010;53:447–57.
[29] Hoare TR. Multi-responsive microgels: synthesis, characterization, and applications; 2006. pp. 1–284.
[30] Roy D, Cambre JN, Sumerlin BS. Future perspectives and recent advances in stimuli-responsive materials. Progr Polym Sci 2010;35:278–301.
[31] Tzoc Torres JMG. Designing dual thermoresponsive & photoresponsive materials for biomedical applications; 2011. pp. 1–110.
[32] Hoare T, Pelton R. Engineering glucose swelling responses in poly(N-isopropylacrylamide)-based microgels. Macromolecules 2007;40:670–8.
[33] Wells LA, Lasowski F, Fitzpatrick SD, Sheardown H. Responding to change: thermo- and photo-responsive polymers as unique biomaterials. Crit Rev Biomed Eng 2010;38:487–509.
[34] Bikram M, West JL. Thermo-responsive systems for controlled drug delivery. Exp OpinDrug Deliv 2008;5:1077–91.
[35] Yin X, Hoffman AS. Poly(N-isopropylacrylamide-co-propylacrylic acid) copolymers that respond sharply to temperature and pH. Biomacromolecules 2006;7:1381–5.
[36] McCoy CP, Brady C, Cowley JF, McGlinchey SM, McGoldrick N, Kinnear DJ, et al. Triggered drug delivery from biomaterials. Exp Opin Drug Deliv 2010;7:605–16.
[37] Christie JG, Kompella UB. Ophthalmic light sensitive nanocarrier systems. Drug Discov Today 2008;13:124–34.
[38] United Nations Environment Health Criteria 23 Lasers and Optical Radiation, United Nations Environment Programme; 1982. pp. 1–191.

[39] Lewis FD, Quillen SL, Hale PD, Oxman JD. Lewis acid catalysis of photochemical reactions. 7. Photodimerization and cross-cycloaddition of cinnamic esters. J Am Chem Soc 1988;110:1261–7.
[40] Ali AH, Srinivasan KSV. Synthesis, characterization, and studies on the solid-state crosslinking of functionalized vinyl cinnamate polymers. J Appl Polym Sci 1997;67:441–8.
[41] Dong C-M, Wu X, Caves J, Rele SS, Thomas BS, Chaikof EL. Photomediated crosslinking of C6-cinnamate derivatized type I collagen, vol. 26; 2005. pp. 4041–9.
[42] Minsk LM, Smith JG, van Deusen WP, Wright JF. Photosensitive polymers. I. Cinnamate esters of poly(vinyl alcohol) and cellulose. J Appl Polym Sci 1959;2:302–7.
[43] Schmidt GMJ. Photodimerization in the solid state. Pure Appl Chem 1971;27:647–78.
[44] Rockel A, Hertel J. Permeability and secondary membrane formation of a high flux polysulfone hemofilter. Kidney Int 1986;30:429–32.
[45] Eriksson L, Johansson E, Kettaneh-Wold M, Wold S. Introduction to multi- and megavariate data analysis using projection methods (PCA & PLS). Introduction to multi- and megavariate data analysis using projection methods (PCA & PLS); 1986. pp. 17–32.
[46] Nichols E. Latent variable methods: case studies in the food industry; 2011. pp. 1–102.
[47] Muteki K, MacGregor JF, Ueda T. Rapid development of new polymer blends: the optimal selection of materials and blend ratios. Ind Eng Chem Res 2006;45:4653–60.
[48] Muteki K, MacGregor JF, Ueda T. Mixture designs and models for the simultaneous selection of ingredients and their ratios. Chemometr Intell Lab 2007;86:17–25.
[49] Ju HK, Kim SY, Kim SJ, Lee YM. pH/temperature-responsive semi-IPN hydrogels composed of alginate and poly(N-isopropylacrylamide). J Appl Polym Sci 2001;83:1128–39.
[50] Dinçer S, Tuncel A, Pişkin E. A potential gene delivery vector: N-isopropylacrylamide-ethyleneimine block copolymers. Macromol Chem Phys 2002;203:1460–5.
[51] Lee SB, Ha DI, Cho SK, Kim SJ, Lee YM. Temperature/pH-sensitive comb-type graft hydrogels composed of chitosan and poly(N-isopropylacrylamide). J Appl Polym Sci 2004;92:2612–20.
[52] Fitzpatrick SD, Mazumder MAJ, Lasowski F, Fitzpatrick LE, Sheardown H. PNIPAAm-grafted-collagen as an injectable, in situ gelling, bioactive cell delivery scaffold. Biomacromolecules 2010;11:2261–7.
[53] Hoare T, Mclean D. Kinetic prediction of functional group distributions in thermosensitive microgels. J Phys Chem B 2006;110:20327–36.